Detection of single-trial events in BOLD fMRI without prior stimulus information

C. Caballero[1], N. Petridou[2], S. Francis[2], I. Dryden[3], L. Bai[1], and P. Gowland[2]

[1]School of Computer Science, University of Nottingham, Nottingham, United Kingdom, [2]Sir Peter Mansfield Magnetic Resonance Center, University of Nottingham, Nottingham, United Kingdom, [3]School of Mathematical Sciences, University of Nottingham, Nottingham, United Kingdom

Introduction: The aim of this work is to map in space and time the brain's response to single stimuli without prior knowledge of when the stimulus occurred**.** Detection of true single-trial events can facilitate the characterization of higher cognitive processes, such as learning or adaptation. However, detection of single-trial events in BOLD fMRI time series is a challenging task especially in the presence of physiological and systematic fluctuations that may impede the detection of BOLD signal changes. Here, a procedure based on Wiener deconvolution is proposed to detect single-trial events with no prior information on stimuli timing. Automatic detection is carried out based on a single assumption of the general shape of the hemodynamic response function (HRF), and employing a simple tissue-dependent noise characterization. Furthermore, this technique allows identification of individual trials, and the temporal/spatial evolution of the BOLD response.

Theory: When modelling fMRI time series as the output of a linear time invariant (LTI) system [1], the time series for a given voxel, $\boldsymbol{x}(\boldsymbol{n})$, is the convolution of the underlying activity, $\boldsymbol{m}(\boldsymbol{n})$, with the hemodynamic response function (HRF), $\boldsymbol{h}(\boldsymbol{n})$, plus an additive stochastic noise, $\boldsymbol{v}(\boldsymbol{n})$. Assuming that the noise follows a Gaussian distribution and under this LTI model, the infinite impulse response (IIR) Wiener filter, $\mathbf{W}(\boldsymbol{f})$, is optimal in order to minimize the mean squared error between the estimate, $\boldsymbol{y}(\boldsymbol{n}) = F^{-1}\{\mathbf{W}(\boldsymbol{f})\mathbf{X}(\boldsymbol{f})\}$**,** and the actual activity, $\boldsymbol{m}(\boldsymbol{n})$. Assuming that the BOLD response is a deterministic signal, the frequency response of the IIR Wiener filter is [2-4]: $\mathbf{W}(f) = \mathbf{A}\mathbf{H}^{*}(f) \Big/ \left(\left| \mathbf{A}\mathbf{H}(f) \right|^{2} + \mathbf{S}_{v}(f) \right)$,where $\mathbf{S}_{\mathbf{v}}(\boldsymbol{f})$ is the spectral density function of $\boldsymbol{v}(\boldsymbol{n})$**,** $\boldsymbol{A}$ denotes the amplitude of a normalized HRF, and * denotes conjugate.

Methods: Noise was modelled as an zero-mean uncorrelated process, i.e. $\mathbf{S}_{\mathbf{v}}(\boldsymbol{f}) = N_0$ [2], considering, however, that noise is proportional to the signal strength and varies accros brain tissues [5]. Thus, baseline volumes, $\boldsymbol{N}_{\mathbf{B}}$, when ideally no BOLD responses occur, were used to estimate the mean signal intensity, $\boldsymbol{S}_{\mathbf{B}}$, and noise variance for each tissue. Consequently, tissue segmentation was performed (SPM5, FIL/UCL) and different noise terms, N_0^{x}, (where x = gray matter, white matter and CSF) were estimated for each tissue as the mean of the variances of the baseline volumes for all voxels per tissue. The Wiener filter was computed for the TR-sampled SPM canonical HRF with standard parameters. The amplitude of the HRF was estimated for each voxel as $\boldsymbol{A}=(1+\boldsymbol{\alpha})\boldsymbol{S}_{\mathbf{B}}$, where $\boldsymbol{\alpha}$ is the minimum expected BOLD change (~2%). Subsequently, Wiener deconvolution was performed for each voxel time series. In order to statistically test the presence of activation, temporal T-statistics were defined from the extracted time series as $\boldsymbol{T}(\boldsymbol{n})=(\boldsymbol{y}(\boldsymbol{n})-\boldsymbol{m}_{\mathbf{B}})/\boldsymbol{\sigma}_{\mathbf{B}}$, where $\boldsymbol{m}_{\mathbf{B}}$ and $\boldsymbol{\sigma}_{\mathbf{B}}$ are the mean and standard deviation of $\boldsymbol{y}(\boldsymbol{n})$ in the baseline volumes, respectively. Hence, T-statistics follow a Student's t-distribution with $\boldsymbol{N}_{\mathbf{B}}$-1 degrees of freedom. The null hypothesis, i.e. that no activation is present, was rejected if the temporal T-statistic exceeded the threshold set by a specified p-value, for each individual time point and voxel. Finally, temporal clustering in addition to spatial clustering (AFNI, NIMH/NIH) was applied on the thresholded time series in order to reduce false positives.

This methodology was tested on three fMRI datasets (single-shot gradient-echo EPI) acquired at 3T and 7T (Philips Achieva). **Dataset 1 – 3T**: Imaging: TR: 2.2s, TE: 40ms, matrix: 64x64, 3.25mm in-plane resolution, 3mm slice thickness, 20 slices, 26 baselines. Paradigm: 8Hz reversing checkerboard, 5s / 30s OFF, 40 cycles. **Dataset 2 - 7T**: Imaging: TR: 2s, TE: 30ms; matrix: 96x96; 2mm in-plane resolution; slice thickness: 2mm, 16 slices, 110 images, 40 baselines. Paradigm: 3 trials of 4s finger-tapping, initiated with a visual cue at 80s, 114s, and 168s of the scan duration. **Dataset 3 – 7T**: Imaging: TR: 400ms, TE =30ms; matrix = 96x96; 2mm in-plane resolution; slice thickness: 2mm, 225 images, 50 baselines. Paradigm: 2 trials of finger-tapping, 2s and 4s respectively, initiated with a visual cue at 20s and 52s of the scan duration. Heart rate (pulse oximeter) and respiration (pneumatic belt) were recorded in all sessions. Datasets were corrected for motion, low frequency drifts and physiological noise (RETROICOR [6]). Data analysis was performed as described above, excluding the voxels classified as CSF.

Results: Figure 1 shows the results for the motor/visual paradigm at 7T with TR=2s. The plotted time series corresponds to a voxel in the premotor cortex. As can be seen, the three trials were correctly detected, while noisy periods (e.g. time point A) were correctly classified as non-activation. On the right, T maps (uncorrected p-value=0.075, 39 d.f.) illustrate the temporal evolution of the detected activity. The first map (A) corresponds to a time point in the baseline period (and is representative of maps obtained between trials). It can be seen that activity is first seen in lateral premotor and supplementary motor areas (SMA) (B,C) which are involved in motor initiation. At a later time (D,E) activity is seen in the sensorimotor cortex. Finally activation occurs in parietal areas (F) which are involved in visuomotor transformations and evaluation of self-generated movements. Similar statistical results were obtained for all datasets.

Conclusion: The results presented show that detection of single-trial events is feasible with no information about stimuli timing, and without averaging, even under the simple assumption of uncorrelated noise. This is achieved by the use of a Wiener deconvolution technique. Furthermore, with this method, the temporal evolution of the BOLD signal changes across and between brain regions is shown. The interpretation of these maps is simpler than the use of ICA. Future work will incorporate a more elaborated noise characterization and address the issue of multiple hypothesis testing.

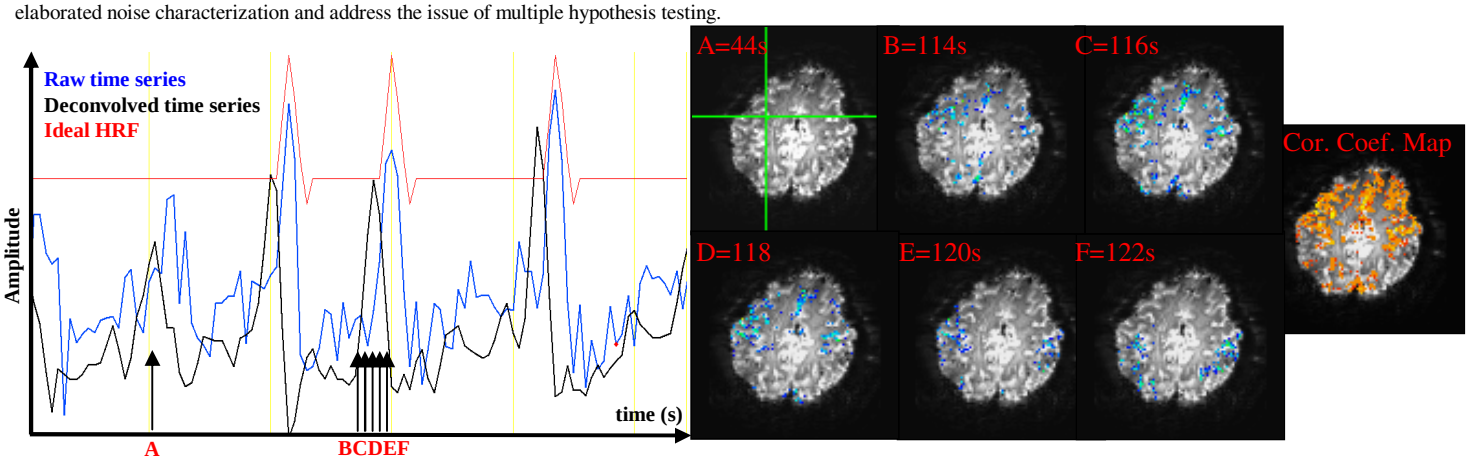

Figure1. Left: Original fMRI time series (blue) and deconvolved time series (black) of a voxel located on the premotor cortex (indicated in map A). The red line represents the HRF convolved with the stimulus function, and it is shown for reference. Right: T-maps for the different time points indicated by arrows on the time series, overlaid on the corresponding EPI image. Activation in premotor, SMA, sensorimotor and parietal cortex was detected along with visual cortex due to the visual cue. For reference, the activation map obtained by correlation with the stimulus function (p=0.01) is shown on the far right.

Acknowledgements: This work is supported by FP6 Marie Curie Action Programme (MEST-CT-2005-021170) and a grant from the MRC and EPRSRC.

References: 1. G.M.Boynton et.al., J.Neuroscience, 1996, 16(13):4207-4221**. 2.** G.Glover, NeuroImage, 1999, 9(4):416-429. **3.** M.H.Hayes, John Wiley&Sons, 1996. **4.** Y.C.Eldar, IEEE Trans. Inf. Theory, 2005, 51(8):2921-2929. **5.** G.Krueger et.al., MRM, 2001, 46:631-637. **6.** Glover et al.., MRM, 2000, 44:162-167.